

# Optimization Design of Key Parameters of Forming Parts of an Involute Plunger Type Biomass Ring Die Pelletizing Machine by DEM-FEM Coupled Modeling

Akang Zhao,<sup>#</sup> Tao Liu,<sup>\*#</sup> Xuehong De, Bowen Zhang, and Xingchen Lv

Due to the complex motion state of biomass raw materials in the granulation process of involute plunger biomass ring mold granulator, it is difficult to analyze by use of a linear mechanical model. Accordingly, a granulation simulation model of molded parts was established by coupling discrete element (DEM) and finite element (FEM) analyses. The stress and strain results of ring die and involute plunger pressure roller were analyzed. On this basis, it can be predicted that for wood pellet materials, when the pressure angle of the involute plunger involute profile is 20°, the ring mold forming hole length-diameter ratio is 4.5, the forming hole diameter is 8 mm, and the hole cone angle is 90°, the compression force on the wood pellet will be maximized at 7.89 KN, the maximum equivalent force at the ring mold forming hole and the root of the involute plunger pressure roller will be 64.2 and 84.5 MPa, respectively, and the maximum deformation will be 0.000327 and 0.000424 mm, which is within permissible limits. The involute plunger roller is more susceptible to fatigue damage compared with the ring die. By contrast, the ring part is more prone to fatigue damage in the case of a ring die.

DOI: 10.15376/biores.18.4.8120-8133

*Keywords:* Discrete element; Finite element; Nonlinear mechanics; Strength analysis; Ring die granulator; Biomass; Fatigue damage

*Contact information:* College of Mechanical and Electrical Engineering, Inner Mongolia Agricultural University, Hohhot, PR China; #: These authors contributed equally to this work;

\* Corresponding author: liutao@imau.edu.cn

## INTRODUCTION

Biomass energy has enormous reserves in nature and can be converted into fuel to compensate for the existing energy shortage and provide diversified security for socio-economic development (Qin 2019). Biomass energy also has the inherent shortcomings of low energy and mass density, which leads to the difficulty and cost increase in collection, storage, and transportation. The biomass ring die pelletizer is a type of biomass energy processing equipment that takes agricultural and forestry production waste (such as wood chips, straw, rice husk, bark, and other biomass) as raw materials, and after crushing and drying to reach the pelletizing conditions, the device forms it into high-density pellet fuel (Ji *et al.* 2020; Gao *et al.* 2021). A ring die pelletizer is a high-efficiency biomass energy conversion equipment, but the ring die and the pressure roller experiences the problem of rapid wear, resulting in decreased pelletizing efficiency and increased energy consumption. A plunger ring die granulator is a new type of ring die granulator. During its operation, a protruding plunger can push the material into the ring die molding hole more efficiently, and it can be adjusted according to the actual production of the plunger and the ring die

into the ring die molding hole depth (De *et al.* 2020). The plunger ring die granulator has the advantages of high production efficiency, wear resistance, and low energy consumption, but it also has the disadvantages of limited granulation pressure and high production cost.

Numerous scholars have conducted studies on biomass pellet granulators. Ning *et al.* (2016) conducted research on the granulation process of plunger ring die granulator, taking microcrystalline cellulose as an example, and adopting the continuous medium mechanics method combined with the built-in Drucker-Prager Cap material ontology of ABAQUS software to carry out numerical simulation and optimization of molding parameters. Li *et al.* (2022) analyzed the flat roll ring die molding machine by discrete element-finite element (DEM-FEM) coupling, and the results showed that the ring die components were more prone to wear compared with the pressure roll components. Chojnacki *et al.* (2019) used the finite element implicit solution method to simulate the contact between the die and the wood chip material of the flat die pelletizer mold and obtained a new optimized structure of the die. Liu *et al.* (2023) used the combination of mechanical model and finite element to analyze the plunger-type pressure roller and showed that changing the plunger from a cylindrical type to a rotary involute type can significantly improve the wear condition and achieve a more uniform force.

For the finite element analysis of the ring die pelletizing components, due to the existence of geometric nonlinearity, material nonlinearity, and boundary condition nonlinearity in the pelleting process, most of the simulation studies in this direction use a single way to simulate, which cannot be more closely matched to the actual simulation of mechanical behavior in the pelleting process, and the results have a large error with the real state (Xu *et al.* 2017; Zhao *et al.* 2021). This paper adopts the coupled method of discrete element (DEM) and finite element (FEM), which can synthesize the advantages of discrete element (DEM) and finite element (FEM) simulation, and organically combine the two simulation methods. Discrete element (DEM) simulates the characteristics of granular materials and analyzes the interaction force between particles and particles; finite element (FEM) simulates the equal strain and deformation of the involute plunger press roll and ring die. By combining discrete elements (DEM) and finite elements (FEM) with each other, the performance of ring die granulation components can be analyzed more accurately.

## EXPERIMENTAL

### **Involute Plunger Type Ring Die Granulator Structure and Molding Principle**

*Key structure and simplified model of involute plunger type ring die granulator molding machine*

The involute plunger-type ring die granulator is composed of a ring die and pressure roller. The ring dies and pressure roller are connected directly with the ring die shaft and pressure roller shaft, and transmission gears are installed on the two shafts to make the ring die and pressure roller rotate in the same direction through the gears on the intermediate shaft, and the power is input through the pressure roller shaft. The pressure roller is distributed uniformly with involute plungers, which bite each other with the molding holes on the ring die during operation. To improve computational efficiency and avoid non-essential calculations, the model was simplified, as shown in Fig. 1. The profile of the

involute plunger was established by the rotary involute molding method with parametric equations in the right-angled coordinate system, as follows,

$$x_i = r_k \cos a_k + r_k a_k \sin a_k \quad (1)$$

$$y_i = r_k \sin a_k + r_k a_k \cos a_k \quad (2)$$

where  $x_i$  is the transverse coordinate of the involute curve,  $y_i$  is the longitudinal coordinate of the involute curve, and  $a_k$  is the pressure angle of the involute curve.

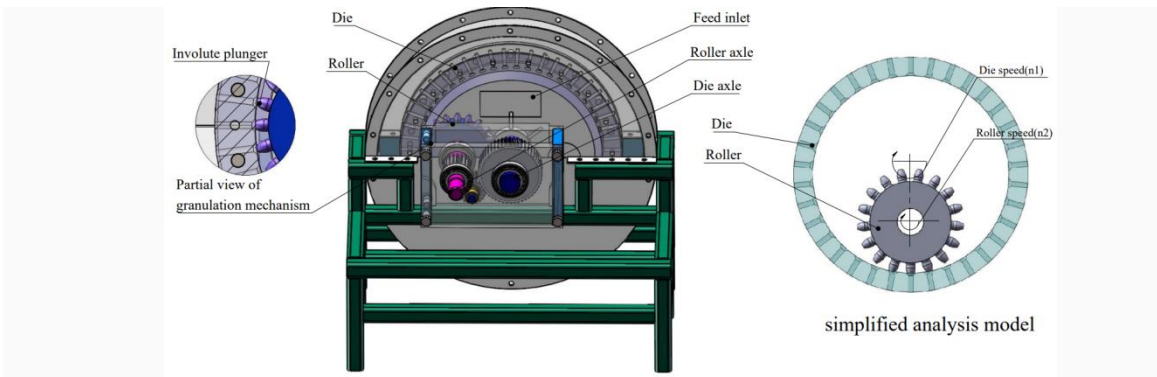


**Fig. 1.** Key structure and simplified model of involute plunger ring die granulator forming machine

#### *Working principle of involute plunger type ring die granulator*

The dried and crushed biomass raw material must be added to the plunger ring die granulator for it to function properly. Similar to how gear and gear ring rotation meshes, the ring die and involute pressure roller rotate in the same direction when powered by the gear set, allowing the material to progressively enter the molding hole of the ring die. In this process, the material particles are combined to form compressed particles, the density gradually rises, and when the material is squeezed by the pressure that is sufficient to overcome friction with the inner wall of the mold hole, the material is extruded out of the ring mold outside of the molding holes. When it reaches the required length, it is cut off by the cutter knife, as shown in Fig. 2.

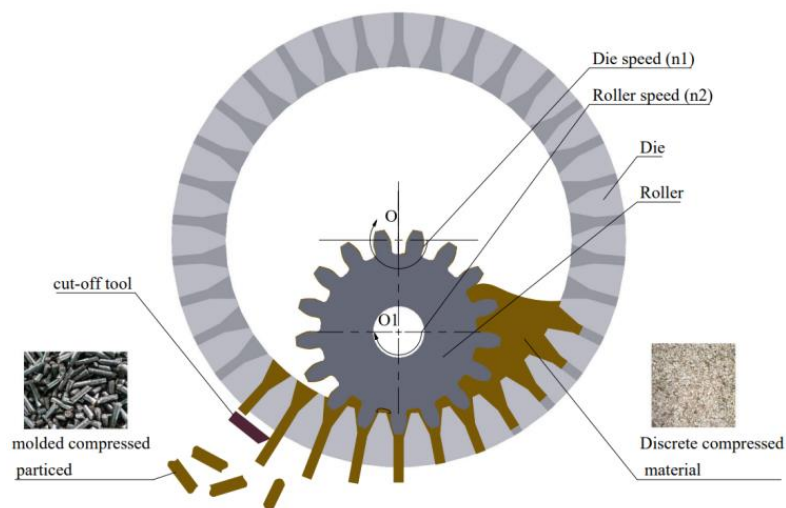


**Fig. 2.** Working principle of involute plunger type ring die granulator

**Theoretical Studies**

*Principles of discrete element method analysis*

The discrete element method divides the research object into mutually independent units and uses iterative methods such as dynamic relaxation method or static relaxation method to carry out cyclic iterative calculations. These calculations determine the forces and displacements of all the units at each time step and updates the positions of all the units. By tracking the microscopic motion of each unit, the macroscopic motion law of the whole research object can be obtained (Cundall and Strack 1980).

The motion between the particles is independent of each other when the particles are in contact with each other. Only when they interact at the contact point, will the particles be considered as a two-dimensional rigid circular particle model. In that case, a three-dimensional rigid spherical model is applied, as shown in Fig. 3. This model is the Hertzian contact model for particle-particle contact.  $R_A$  and  $R_B$  are the circle radii of particle A and particle B, respectively,  $a$  is the contact circle radius, and  $\delta$  is the contact deformation. The particle model of the discrete element method simulates the particle-particle and particle-boundary contact using vibration equations of motion. Figure 3 represents the model as a vibration model, and the normal and tangential motion of vibration motion is shown in the normal and tangential vibration model in Figs. 4(a) and 4(b), and the sliding between the particle-particle and particle-boundary is shown in the sliding model in Fig. 4(c).

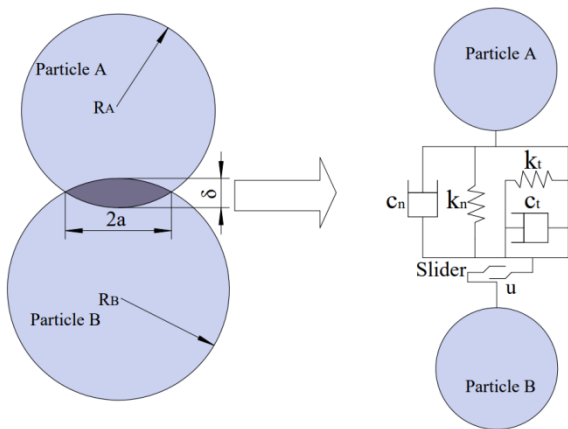


**Fig. 3.** Contact model expressed as a vibration model

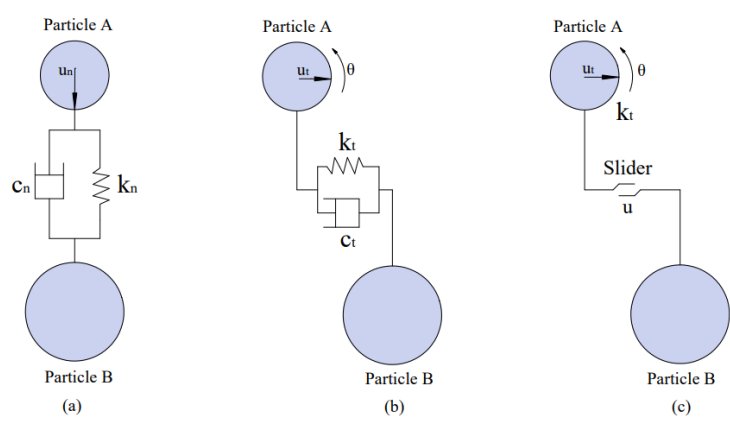


**Fig. 4.** Normal vibration model, tangential vibration motion model, and sliding model

The vibratory motion of the particle contact process is decomposed in normal and tangential directions, and the normal vibratory motion equation of the particle contact process is:

$$\frac{m_{A,B}d^2u_n}{dt^2} + \frac{c_n du_n}{dt} + k_n u_n = F_n \tag{3}$$

The tangential vibratory motion of the particle contact process is manifested as tangential sliding with rolling of the particles,

$$\frac{m_{A,B}d^2u_t}{dt^2} + \frac{c_t du_t}{dt} + k_t u_t = F_t \tag{4}$$

$$\frac{I_{A,B}d^2\theta}{dt^2} + \left( \frac{c_t du_t}{dt} + k_n u_t \right) s = M \tag{5}$$

where  $m_{A,B}$  is the equivalent mass of particles A and B, and  $I_{A,B}$  is the equivalent rotational inertia of the particles. The parameter  $s$  is the rotational radius, and  $u_n$  and  $u_t$  are the normal and tangential relative displacements of the particles, respectively. The angle  $\theta$  is the rotational angle of the particles themselves;  $F_n$  and  $F_t$  are the normal and tangential components of the external forces on the particles, respectively;  $M$  is the external moment of the particles;  $k_n$  and  $k_t$  are the normal and tangential elasticity coefficients in the contact model; and  $c_n$  and  $c_t$  are the normal and tangential damping coefficients in the contact model.

Both tangential sliding and rolling of particles are affected by the friction force between particles. The limit conditions of tangential sliding and rolling of particles can be established by the sliding model (Burns *et al.* 2019).

$$F_n = uk_n u_n \text{sgn} \left[ k_t \left( u_t + \frac{d\theta}{2} \right) \right] \quad (6)$$

where  $u$  is the friction coefficient of the particle;  $\text{sgn}[]$  is a symbolic function, and  $\text{sgn}(x) = \begin{cases} 1 & x \geq 0 \\ -1 & x < 0 \end{cases}$ .

According to the force-displacement relationship, the force on the particle can be obtained from the displacement. From Newton's second law, the equation of motion of the particle is obtained as follows,

$$\begin{cases} m_i \ddot{u}_i = \sum F \\ I_i \ddot{\theta}_i = \sum M \end{cases} \quad (7)$$

where  $\ddot{u}_i$  and  $\ddot{\theta}_i$  are the acceleration and angular acceleration of particle  $i$ ,  $m_i$  and  $I_i$  are the mass and rotational inertia of particle  $i$ , and  $\sum F$  and  $\sum M$  are the combined external force and the combined external moment of the particles at the center of mass.

Numerical integration of  $\sum F$ ,  $\sum M$  is carried out by the center difference method, and the update rate expressed by the center of two-time steps is obtained as,

$$\begin{cases} (\dot{u}_i)_{N+\frac{1}{2}} = (\dot{u}_i)_{N-\frac{1}{2}} + \left[ \sum \frac{F}{m_i} \right]_N \Delta t \\ (\dot{\theta}_i)_{N+\frac{1}{2}} = (\dot{\theta}_i)_{N-\frac{1}{2}} + \left[ \sum \frac{M}{I_i} \right]_N \Delta t \end{cases} \quad (8)$$

where  $\Delta t$  is the time step;  $N$  corresponds to the time  $t$ .

Integrating the above equation yields the equation for displacement:

$$\begin{cases} (u_i)_{N+1} = (u_i)_N + (\dot{u}_i)_{N+\frac{1}{2}} \Delta t \\ (\theta_i)_{N+1} = (\theta_i)_N + (\dot{\theta}_i)_{N+\frac{1}{2}} \Delta t \end{cases} \quad (9)$$

The new displacement value of the particle is obtained, and this new displacement is substituted into the force-displacement relationship to calculate the new force, and the cycle is repeated to realize the tracking of the motion of each particle at any moment.

*DEM-FEM coupled model*

The discrete element method (DEM) is unable to simulate the equivalent stresses and strains of the ring die and the involute plunger rollers after the pelletizing process of discrete biomass particles, and finite elements are needed to calculate the equivalent stresses and strains. When analyzing the interaction between particles and components using the DEM-FEM coupling method, the load of discrete element particles on components is transferred to the finite element analysis model as a boundary condition of the finite element analysis, which is used to calculate the distribution of the constructed stress field and displacement field. According to the discrete element analysis output model loads on each node, when the imported model is composed of a series of triangular face sheets, the output load matrix is,

$$P_i = [x_i, y_i, z_i, F] \quad (10)$$

where  $P_i$  is the force applied to the unit node  $i$ ;  $x_i, y_i, z_i$  are the coordinates of the unit node  $i$ ; and  $F$  is the load value of the unit node  $i$ .

The dynamic implicit solution is used to define the equilibrium in the form of applied external force  $P$ , internal force  $I$  in the unit, and node acceleration as,

$$M\ddot{u} = P - I \quad (11)$$

where  $M$  is the mass matrix and  $\ddot{u}$  is the unit node acceleration.

Based on the full Newton iterative solution method, iterations are performed using automatic incremental steps to form the tangent stiffness matrix, and at the end of the incremental step at the moment  $t + \Delta t$ , the Newton iterative solution seeks to satisfy the conditions of the dynamic equilibrium equations. Based on the material intrinsic model, the stress, displacement increment, strain, and fatigue life curves of the member are calculated. Figure 5 shows the flow chart of the coupled DEM-FEM numerical analysis framework.

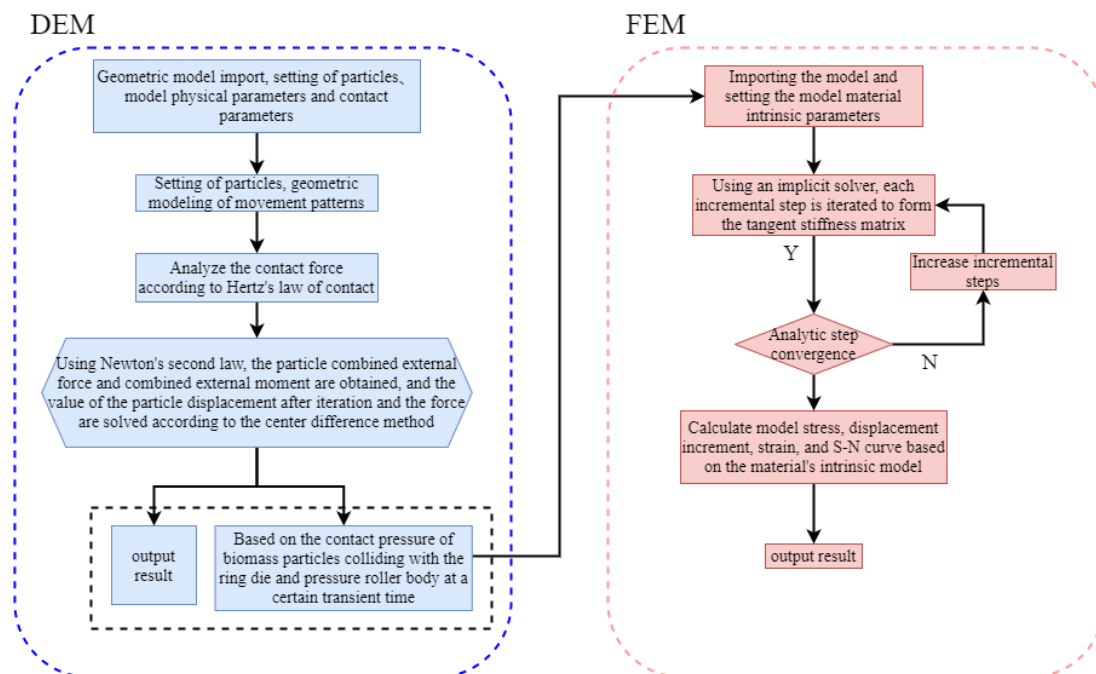


**Fig. 5.** Flow of the coupled DEM-FEM numerical analysis framework

## RESULTS AND DISCUSSION

### Discrete Element Modeling and Simulation of the Material Compression Process

#### *Discrete element EDEM model simulation variable setting*

The simulation was specified with the involute plunger involute contour pressure angle set to  $20^\circ$  in the involute plunger top and ring mold molding hole distance of 1.5 mm, the ring mold molding hole length to diameter ratio of 4.5, the molding hole diameter of 8 mm under the conditions of the conditions, respectively, into the hole cone angle of  $60^\circ$ ,  $90^\circ$ , and  $120^\circ$  when the simulation of the motion simulation.

The flexible body model of the simulation model ring die and involute plunger pressure roller was imported into EDEM, the boundary conditions were set, and the two were set to rotate around their geometric centers. The mold-roll ratio of the ring mold and the pressure roller was 2. The rotational speed of the ring mold was 360 deg/s, that of the pressure roller was 720 deg/s, and the acceleration was zero. For the biomass material, the shape after crushing was similar to the needle shape, and the particle size was between 2 and 5 mm, so the simulation material model was selected to have a length of 3 mm. A single material entity was constructed by direct modeling, with six spheres of radius 0.5 mm in series with each other, as shown in Fig. 6. The ring mold, pressure roller, and biomass material intrinsic model are shown in Table 1.

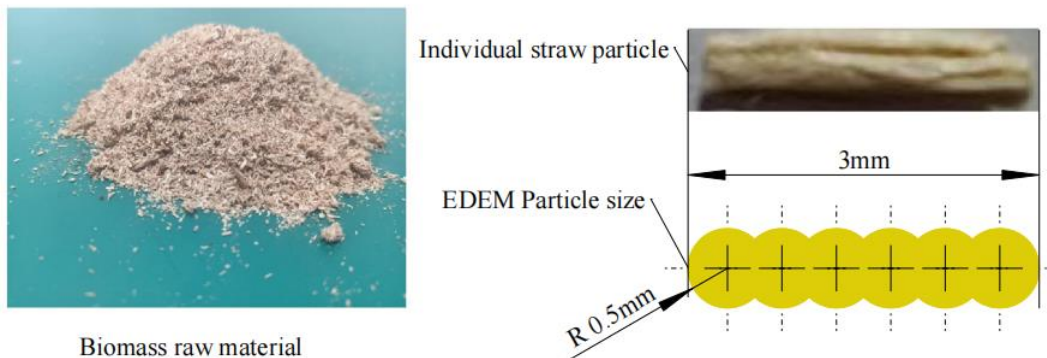


**Fig. 6.** Discrete element simulation particle

**Table 1.** Discrete Element Simulation Material Parameter Settings

Simulation Material	Shear Modulus (MPa)	Poisson Ratio	Density ( $\text{kg/m}^3$ )
Ring Die and Roller(42CrMo)	$8e^4$	0.3	7850
Biomass Materials (Wood Chips)	$7e^{-1}$	0.25	290

The definition of ring mold and pressure roller contact parameters refers to commonly used structural steel material settings. After reviewing the relevant literature, biomass material parameters were determined by their nature, the type of material, moisture content, particle size, *etc.*, in order to derive the contact parameters of the discrete element simulation in this paper, as shown in Table 2.

**Table 2.** Contact Parameter Settings for Discrete Element Simulation

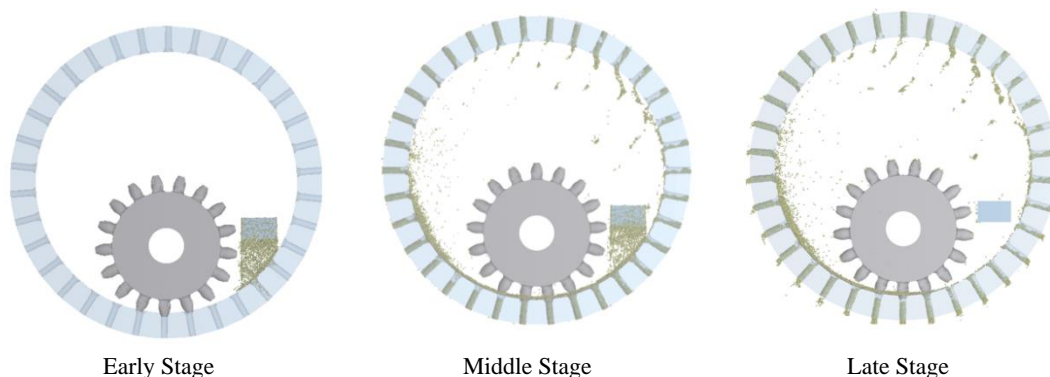
Contact Type	Coefficient of Restitution	Static Friction Coefficient	Kinetic Friction Coefficient
Particle-Particle,	0.42	0.47	0.13
Particle-Flexor Models	0.52	0.45	0.05

#### *Discrete element contact modeling setup*

The choice of contact model should be based on the actual situation of biomass molding. In this paper, particle-to-particle contact is selected from the contact models built into the analysis software, including the Hysteretic Spring model and the Hertz-Mindlin with bonding model. When the biomass material is densely molded, the material particles are plastically deformed under the extrusion and friction of the molding die, lapped and entangled with each other, and broken and embedded, which is in line with the application of the Hysteretic Spring model. The Hertz-Mindlin model can bond spheres together and can be used to bond a limited number of particles of a certain size into a larger particle. The Hertz-Mindlin (no slip) model, which is the basic model for conventional particle contact interaction, was chosen for particle contact with the flexible body model, and the length of the analysis was set to 4 s.

#### *Biomass particle motion analysis*

The involute plunger ring die granulator presents different motion states during the discrete element simulation process. At the beginning of the simulation process, the discrete biomass material generates particles on the right side and falls into the ring die molding holes under the influence of gravity, and the particle movement speed gradually increases. In the middle of the simulation process, the ring die rotates in the same direction as the pressure roller, and the involute plunger on the body of the pressure roller pushes the generated discrete biomass particulate material into the forming hole of the ring die. With the increase of the number of particles in the molding hole, the pressure in the molding hole gradually increases. At the same time, the biomass material has a certain water content, which will lead to the adhesion of some biomass particles on the inner wall of the ring mold. At a later stage of the simulation process, when the squeezing force on the molded particles inside the molding hole is greater than the friction between the outer wall of the molded particles and the inner wall of the molding hole, the particles are extruded out of the molding hole to form hard biomass particles. The pre, mid, and post stages of biomass pellet molding are shown in Fig. 7.

**Fig. 7.** Biomass particle motion analysis

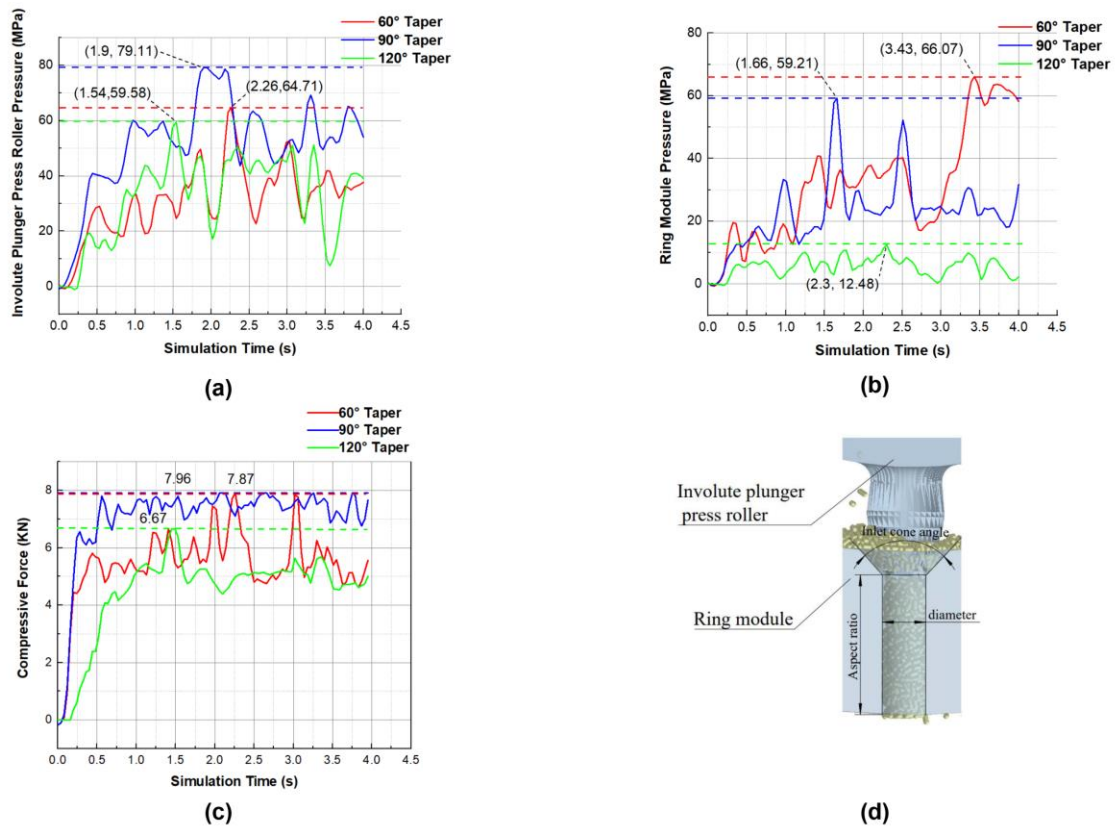


**Fig. 8.** Involute plunger, ring mold force and particle compression force analysis

#### *Simulation model force and molded particle extrusion pressure analysis*

In the simulation, the involute plunger profile curve with the following parameters, the ring mold forming hole diameter and  $L/D$  ratio, are set as fixed parameters, while the ring mold forming hole taper is taken as a variable parameter. As shown in Fig. 8(a), with the movement of the involute plunger, the pressure subjected to gradually increases. When the molding hole entry cone angle is  $60^\circ$ ,  $90^\circ$ , and  $120^\circ$ , the pressure on the involute plunger pressure roller is predicted to be 59.6, 79.1, and 64.7 MPa, respectively. The pressure exerted on the involute plunger rollers in the process of movement mainly comes from the compressed biomass particles in the molding holes, and the size of the pressure exerted is affected by the number and tightness of the particles pressed into the molding holes. Whether the cone angle of forming hole is too large or too small will affect the ability of the particles into the ring mold forming hole, but this will also have a negative impact on the density of biomass particles.

The forces on the ring die also come mainly from the compressed particles inside the molding holes, while the discrete biomass particles that do not enter the molding holes of the ring die have little effect. As shown in Fig. 8(b), the pressure on the ring die increases gradually with the increase of the movement time, and the maximum pressure on the ring die is predicted to be 66.07, 59.21, and 12.48 MPa when the cone angle of the molding hole entry is  $60^\circ$ ,  $90^\circ$ , and  $120^\circ$ , respectively. When the hole cone angle of the molding hole is  $60^\circ$ , the pressure on the ring mold is predicted to reach a maximum value of 20 MPa in the first period, to rise to 40 MPa or so in the middle period, and to continue to increase to 60 MPa or so in the late period, with a greater than  $90^\circ$  and  $120^\circ$  taper hole. When the

hole cone angle of the molding hole is  $90^\circ$ , the pressure of the ring die is predicted to gradually stabilize at about 30 MPa. In the process of movement, there will be two peak values, but which are still far less than the yield limit of the ring die material itself. When the cone angle of the molding hole is  $120^\circ$ , the biomass particles will not enter the molding hole due to the excessive entry cone angle. This will cause the number of particles in the molding hole to be insufficient, and the pressure on the molding hole will be too small, which is not conducive to the molding of the biomass particles.

For biomass pellets, the higher the compression force, the better for pellet molding, which can greatly improve the molding quality of biomass pellets. As shown in Fig. 8(c), the maximum compression forces are predicted as 7.71, 7.89, and 7.30 KN at the molding hole cone angles of  $60^\circ$ ,  $90^\circ$ , and  $120^\circ$ , respectively. When the cone angle of the molding hole is  $90^\circ$ , molding particles are subjected to the largest compression force, and relatively stable, and very conducive to biomass particle molding. Too large or too small cone angle will adversely affect the particle molding, so the  $90^\circ$  cone angle molding effect is greater than the other two cone angle cases. Figures 8(d) shows a schematic diagram of the discrete element simulation.

## Finite Element Strength Analysis

### *Strength analysis of molding parts*

By simulating the biomass pellet molding process, the pellets will generate loads on the plunger, pressure roller, and ring die. In this analysis, discrete element data and finite element data are combined by coupling the EDEM module and Static Structural module in ANSYS Workbench, as shown in Fig. 9.

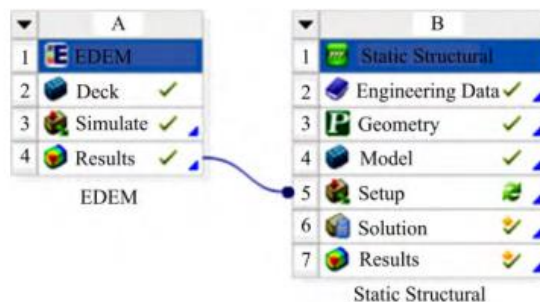


**Fig. 9.** EDEM module coupled with Static Structural module

The coupling file exported after the EDEM calculation was connected to the Static Structural module for coupling through the EDEM module in ANSYS Workbench. From Figs. 8 (a) and (b), it can be concluded that the maximum force generated by the particles on the involute plunger, pressure roller, and ring die will be at 1.90 and 1.66 s, respectively. The time period force information files were exported from EDEM and transferred to the Static Structural module, and the deformation and equivalent force maps of the involute plunger pressure roller and ring die were obtained by solving the mesh (see Figs. 10 and 11). With the ring mold and involute plunger pressure roller continuously engaged in the operation, the materials in the molding area continued to enter the ring mold molding holes, the pressure in the molding hole continued to rise. The ring mold was subject to the maximum equivalent force of 64.2 MPa, and the maximum deformation of the ring mold molding holes at the maximum deformation of 0.000327 mm. The pressure is predicted to

decrease from the molding hole position, and it can be assumed that the pressure on the ring die comes from the pellet and the involute plunger pressure roller, as shown in Fig. 10. The maximum equivalent force on the involute plunger roller is predicted to be 84.5 MPa, and the maximum deformation is predicted to be 0.000424 mm. The force on the involute plunger roller is concentrated in the root area of the involute plunger roller, which can be regarded as a site of bending fatigue damage. Therefore, the root size can be appropriately enlarged, for the involute plunger roller, the force mainly originated from the compressed material in the ring mold forming hole, as shown in Fig. 11.

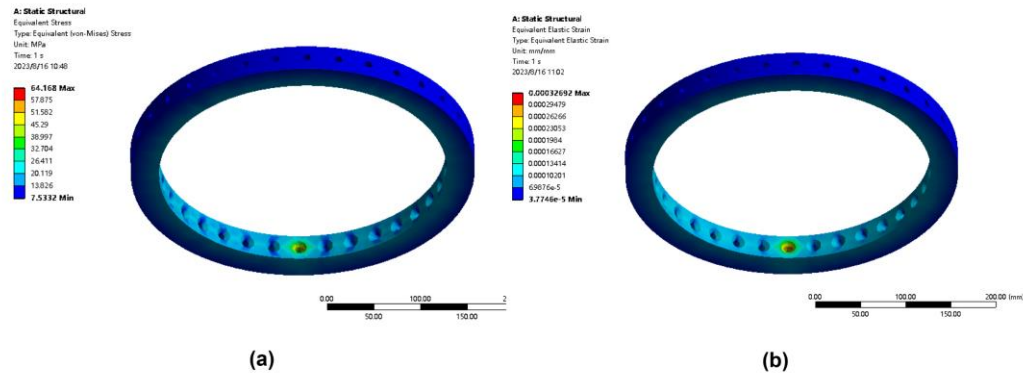


Fig. 10. Cloud diagram of ring mold equivalent force (a) and deformation (b)

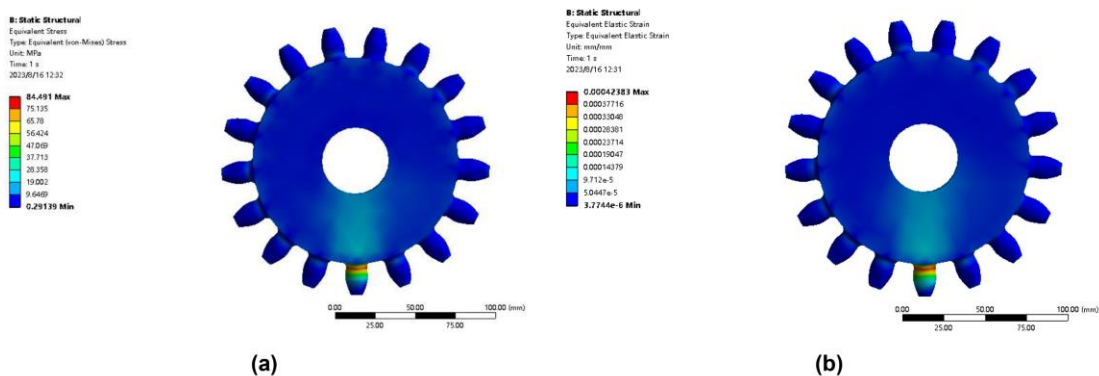


Fig. 11. Cloud diagram of equivalent force (a) and deformation (b) of the involute plunger pressure roller

### Fatigue life analysis of molding parts

In the working process of the ring die forming machine, the ring dies and the pressure roller will be continuously affected by the friction squeezing pressure between the pressure roller and the material, which leads to the cyclic fatigue bending stress and fatigue contact compression stress of the ring die and the pressure roller, and ultimately leads to their fatigue damage (Xue 2014). According to the actual working condition of the ring molding machine, it can be classified as high-frequency cyclic fatigue. Thus, the loading fatigue analysis method was used for the study.

By using the fatigue analysis software, it is possible to solve for the life and damage results for the ring die and involute plunger roll materials and obtain their fatigue life curves as shown in Fig. 12. From the figure, it can be seen that the initial cycle life of both the ring die and the involute plunger press roll was predicted to be  $10^6$  cycles, and the minimum

cycle life decreased to 530,000 cycles and 136,000 cycles respectively when the loading load is 1.5 times the initial load. This indicates that involute plunger rolls are more susceptible to fatigue damage than ring dies. The ring die is an easily damaged part for the conventional flat roller press roll ring die molding machine. However, the cost of replacing the ring die is high, so to reduce the cost of pelletizing, the new idea of converting the wear part from the ring die to the plunger roll will be of great significance.

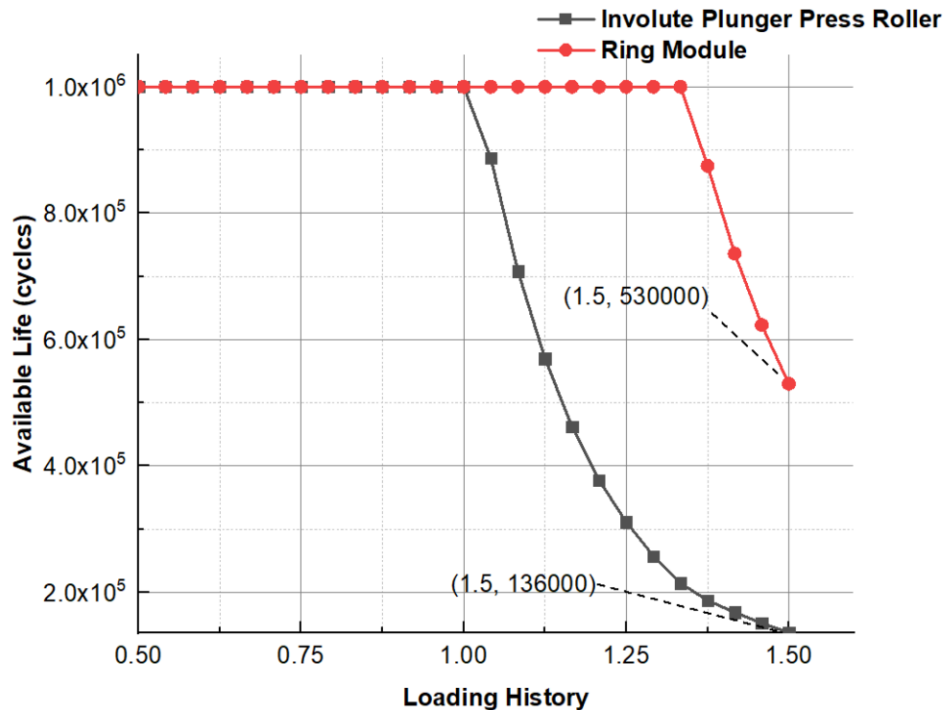


Fig. 12. Fatigue life curve of ring die and involute plunger pressure roller

## CONCLUSIONS

In this paper, the discrete element (DEM)-finite element (FEM) coupling simulation method was applied to simulate the involute plunger ring die molding machine. This approach solves the problem that a single discrete element method simulation method cannot accurately simulate the stresses and strains of the ring die, whereas the involute plunger pressure roller and the finite element method analysis cannot accurately simulate the load generated by the compression of granular parts. By combining these methods, the simulation results come closer to the actual situation. The analysis was based on the use of wood chips particles as the biomass raw material, the use of discrete element method to simulate, and consideration of the involute plunger involute contour pressure angle of 20°, ring mold forming hole diameter of 8 mm, length to diameter ratio of 4.5 conditions, and three kinds of different molding hole into the hole cone angle. Conclusions were drawn as follows:

1. When the cone angle of the molding hole is 90°, the extrusion pressure on the biomass pellets will reach the maximum value. At the same time, too large or too small cone angle of the molding hole will have an effect on the material entering into the molding hole, thus affecting the molding effect of compressed pellets.
2. Through the coupled simulation of the EDEM-ANSYS Workbench, the equivalent force and deformation diagrams of the ring die and involute plunger roller was obtained, and the fatigue life curves of the ring die and involute plunger roller materials were established. The results showed that the ring die molding hole area and the root position of the involute plunger roll are subjected to the largest force, but they are within the permissible range. The load on the ring die molding hole is mainly from the force of the compressed particles, and at the same time the involute plunger roll is more prone to bending fatigue damage compared with the ring die.
3. Replacing the traditional plunger with an involute plunger can change the worn parts from the ring die to the plunger pressure roller, compared with the flat pressure roller ring die pelletizing machine in which the life of the ring die is less than the life of the pressure roller, thus reducing the operating cost of the pelletizing machine. In the future, the design idea of involute gears can be borrowed, by adjusting the pressure angle of the involute tooth profile, in-depth study of the force state of the involute plunger in the process of granulation, and better optimization of the design.

## ACKNOWLEDGMENTS

The authors are grateful to Tao Liu from Inner Mongolia Agricultural University, Hohhot, China, for help with laboratory analysis work. The authors are also grateful for the financial support of the National Natural Science Foundation of China (NSFC) project (51766016) and Research Program of science and technology at Universities of Inner Mongolia Autonomous Regio ( NJZZ23041 )

## REFERENCES CITED

- Burns, S. J., Piiroinen, P. T., and Hanley, K. J. (2019). "Critical time step for DEM simulations of dynamic systems using a Hertzian contact model," *International Journal for Numerical Methods in Engineering* 119(5), 432-451. DOI: 10.1002/nme.6056
- Chojnacki, J., Kaldunski, P., Nagnajewicz, S., and Patyk, R. (2019). "Simulation tests of pelleting process in aspect of obtained stresses, contact pressure and fatigue strength for granulator flat die," in: *Engineering Mechanics 2018*, 24<sup>th</sup> International Conference Proceedings, paper 274. DOI: 10.21495/91-8-157
- Cundall, P. A., and Strack, O. D. L. (1980). "A discrete numerical model for granular assemblies," *Géotechnique* 30(3), 331-336. DOI: 10.1680/geot.1980.30.3.331
- De, X. H., Wu, G. F., Li, N. D., Zhang, J. C., Guo, W. B., and Li, Z. (2020). "Design and testing of an internal mesh planetary wheel plunger-type biomass ring molding machine," *Journal of Agricultural Machinery* 51(10), 379-386. DOI: 10.6041/j.issn.1000-1298.2020.10.043

- Gao, X. Z., Lu, X. T., Nie, J., and Chen, J. (2021). "Biomass pellet fuel production and utilization," *Renewable Resources and Circular Economy* 14(08), 36-39. DOI: 10.3969/j.issn.1674-0912.2021.08.011
- Ji, Y., Li, Y., and Li, H. (2020). "Study of key structure parameters on productivity of the ring-die biomass granulator," *IOP Conference Series: Earth and Environmental Science* 467(1), article 012054 (6pp). DOI: 10.1088/1755-1315/467/1/012054
- Li, Z., Li, J. D., Sha, Q. Y., Yu, Y., Yu, J., and Gao, Y. D. (2022). "Life analysis of biomass molding die based on discrete element-finite element coupling," *Forging Technology* 47(08), 171-177. DOI: 10.13330/j.issn.1000-3940.2022.08.026
- Liu, T., Zhao, A. K., and De, X. H. (2023). "Test and analysis of involute plunger for biomass plunger ring die pelletizing machine," *Feed Industry* 44(05), 8-13. DOI: 10.13302/j.cnki.fi.2023.05.002
- Ning, T. Z., Yu, G. S., Liu, W. G., Jin, S., Yang, H. J., and Zhou, Y. (2016). "Numerical simulation of plunger type pressure roller ring die granulation technology," *Journal of Plasticity Engineering* 23(02), 148-154. DOI: 10.3969/j.issn.1007-2012.2016.02.026
- Qin, J. W. (2019). "Prospects of biomass pellet mill from the perspective of promotion and appraisal," *Agricultural Machinery Quality and Supervision* (01), 17-18+16. DOI: CNKI:SUN:NJST.0.2019-01-010
- Xu, G. Y., Gao, H. F., Huang, G. W., and Zhou, D. W. (2017). "Simulation on the compression molding process of biomass material," *Key Engineering Materials* 748, 456-460. DOI: 10.4028/www.scientific.net/KEM.748.456
- Xue, B. (2014). *Study on the Influence of Structural Parameters of Ring Mold of Biomass Molding Machine on its Life and Molding Quality*, Ph.D. Dissertation, Inner Mongolia University of Science & Technology, Hohhot, China. DOI: 10.7666/d.D517167
- Zhao, H., Huang, Y., Liu, Z., Liu, W., and Zheng, Z. (2021). "Applications of discrete element method in the research of agricultural machinery: A review," *Agriculture* 11(5), article 425. DOI: 10.3390/agriculture11050425

Article submitted: August 30, 2023; Peer review completed: September 30, 2023;  
Revised version received and accepted: October 5, 2023; Published: October 12, 2023.  
DOI: 10.15376/biores.18.4.8120-8133